Tropical Plants

ARTICLE

Open Access

https://doi.org/10.48130/tp-0024-0049

Tropical Plants **2025**, 4: e020

Structural characterization and immunological function of a neutral polysaccharide from *Areca catechu* L. kernels

Authors

Jing Zhang, Xuejie Feng*, Jiahui Dai, Shiping Wang, Xiaoning Kang, ...

Correspondence

13807680898@163.com

In Brief

A homogeneous neutral polysaccharide AKP was extracted from the kernels of Areca nut. The →4)-*β*-D-Manp-(1→ serves as the principal structural component forming the main chain of AKP, and the branched chain is mainly composed of *α*-D-Galp-(1→ attached to the O-6 position of →4,6)-*β*-D-Manp-(1→. AKP attenuates inflammation by regulating the TLR4/NF-*κ*B pathway, decreasing the expression of TLR4, P65, IkB-*α*, MyD88, and inhibiting the release of NO, TNF-*α*, IL-6, and IL-1*β*.

Graphical abstract

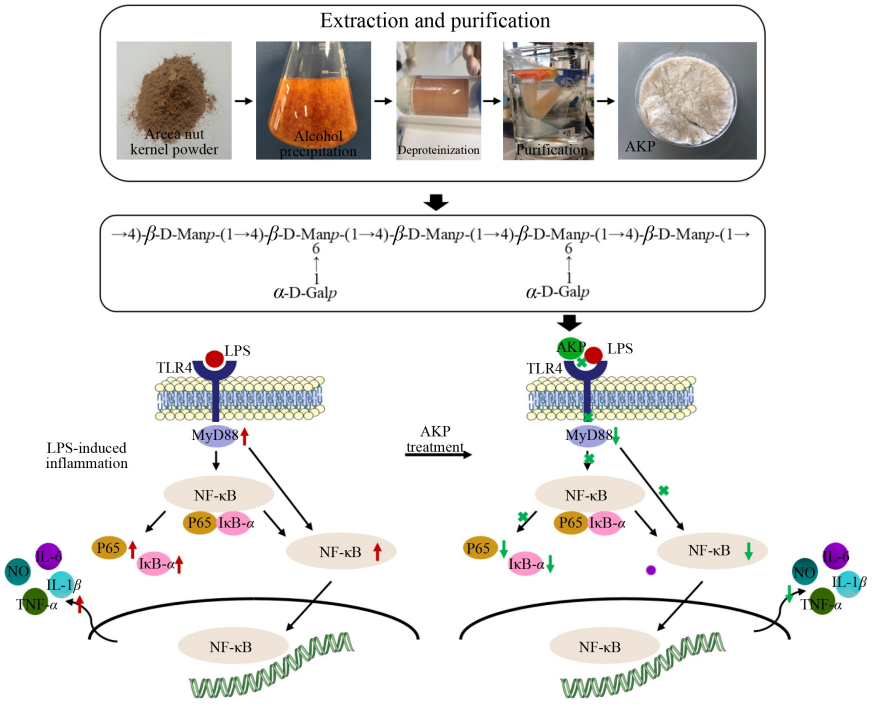

Highlights

- AKP is a homogeneous polysaccharide with a molecular weight of 6.95 × 105 Da.
- The main chain of AKP is mainly composed of →4)-*β*-D-Manp-(1→, and the branched chain is mainly composed of *α*-D-Galp-(1→ attached to the O-6 position of →4,6)-*β*-D-Manp-(1→.
- AKP inhibits the release of NO, TNF-*α*, IL-6, and IL-1*β* in inflammation cells.
- AKP mitigates LPS-induced inflammation by regulating the TLR4/NF-*κ*B pathway.

Citation: Zhang J, Feng X, Dai J, Wang S, Kang X, et al. 2025. Structural characterization and immunological function of a neutral polysaccharide from *Areca catechu* L. kernels. *Tropical Plants* 4: e020 https://doi.org/10.48130/tp-0024-0049

Tropical Plants

ARTICLE

Open Access

https://doi.org/10.48130/tp-0024-0049

Tropical Plants **2025**, 4: e020

Structural characterization and immunological function of a neutral polysaccharide from *Areca catechu* L. kernels

Jing Zhang[1], Xuejie Feng[1*], Jiahui Dai[2], Shiping Wang[2], Xiaoning Kang[2], Wenting Dai[2] and Jianbang Ji[1]

[1] *Sanya Institute, Hainan Academy of Agricultural Science, Sanya 572000, Hainan, PR China*

[2] *Institute of Processing & Design of Agriproducts, Hainan Academy of Agricultural Science, Haikou 570100, Hainan, PR China*

* Corresponding author, E-mail: 13807680898@163.com

Abstract

Areca nut kernels are the byproduct of areca nut processing. Some of the major bioactive components of the areca nut are polysaccharides. Polysaccharides are known to exert numerous biological activities. Thus, polysaccharides isolated from areca nut kernels may be clinically valuable. To determine the medicinal value of areca nut kernel polysaccharides (AKP), ultrasonic-assisted extraction, ethanol precipitation, and dialysis were used for separation and purification. SEM, XRD, FTIR, and NMR were used for structural characterization and RAW264.7 macrophages were used for in *vitro* immune activity assessment. The AKP were isolated was a neutral polysaccharide, and the molecular weight (M*w*) was 6.95×10^5 Da, primarily composed of mannose (58.7%) and galactose (33.6%); the main chain of AKP is →4)-β-D-Man*p*-(1→, and the branched chain was mainly of α-D-Gal*p*-(1→ attached to the O-6 position of →4,6)-β-D-Man*p*-(1→. Cell experiments show that AKP (20 μg/mL) exerts its immune function *via* the TLR4/NF-κB signaling pathway regulation, decreasing TLR4, P65, IκB-α, and MyD88, and reducing the release of TNF-α, NO, IL-6, and IL-1β. In addition, AKP immune activity might be ascribed to its high M*w* and rich monosaccharide composition. This study offers a solid scientific foundation for the development of AKP for wide clinical application.

Citation: Zhang J, Feng X, Dai J, Wang S, Kang X, et al. 2025. Structural characterization and immunological function of a neutral polysaccharide from *Areca catechu* L. kernels. *Tropical Plants* 4: e020 https://doi.org/10.48130/tp-0024-0049

Introduction

The tropical palm tree, *Areca catechu* L., is widely planted in southern and southeast Aisa as well as in the tropical and subtropical areas in the south of China[1]. Areca nut (AN) chewing is regarded as an ancient custom[2]. It is reported that over 400 million individuals chew AN globally[3].

In China, there are two main ways in which AN is consumed: chewing fresh AN (contains AN, betel leaf, and slaked lime) and chewing processed AN (accounting for 95% of consumption). AN processing involves the addition of additives such as flavoring agents and sweeteners. AN is processed mainly using the following methods: boiling of seeds, roasting of seeds, smothering the aroma, pressing the seeds, cutting the seeds, removing the kernels, and spotting the brine. Thus, AN is processed through kernel removal, and the removed kernels are discarded. In fact, only 1% of AN is used for fresh consumption, and about 95% of AN are processed into chewing blocks for human consumption. Based on the volume of AN products processed, this means that the amount of discarded AN kernels is significant. Therefore, it is important to explore the value of AN kernels.

AN kernels contain polyphenols, alkaloids, fatty acids, polysaccharides, trace elements, and other active ingredients[4]. Polysaccharides are natural high-molecular weight polymers, which are formed by several monosaccharide residues connected through glycosidic bonds[5]. Polysaccharides exhibit various bioactivity functions, such as anti-oxidation, immune regulation, tumor suppression, anti-aging, and anti-diabetic activity[6]. AN kernels serve as a source of polysaccharides.

A polysaccharide content of 18.7% has been reported in AN. To date, the studies on AN polysaccharides have mainly focused on the optimization of extraction process and *in vitro* antioxidant activity. It has been reported that a crude extract of AN polysaccharide had an inhibitory effect on oxidative damage in human skin fibroblasts. It had good scavenging ability for DPPH, ABTS+ and OH, exhibiting good antioxidant activity[7–9]. According to Hu et al., the monosaccharide composition of *Areca catechu* seed polysaccharides are mannose, glucose, and galactose[10]. The molecular weight of AK polysaccharides was 1.84×10^4 to 4.79×10^5 g/mol. They also indicated AK contained extracted polysaccharides which exhibited strong antioxidant activity. Ji et al. obtained a novel neutral polysaccharide from AN, with a M*w* of 37.3 kDa. The backbone of the polysaccharide was composed of →6-β-Man*p*-(1→, →4)-α-Gal*p*-(1→ and →3,6)-β-Man*p*-(1→) residues[11]. PAP1 exhibits antioxidant activity, based on DPPH and OH scavenging ability. However, there is limited information regarding structural information and immune function of polysaccharides isolated from AN kernels.

Therefore, in this study, the aim was to extract AN kernels polysaccharides (AKP) using water extraction and ethanol precipitation. In addition, the aim was to purify the extracted AKPs using dialysis and perform AKP structural characterization. Furthermore, the immune function of AKP was investigated by using RAW 264.7 cell, including cell viability, NO released, TNF-α released, IL-6 released, IL-1β released, and pathways for exerting anti-inflammatory effects. This study provide a theoretical basis for further research of AN, paving the way for AN kernel's further development and utilization in medical fields.

Materials and methods

Materials

Areca nut kernels were collected from Haikou Areca Processing Research Key Laboratory, Institute of Processing & Design of Agriproducts, Hainan Academy of Agricultural Science (Hainan, China). RAW264.7 murine macrophages were purchased from Huayan Biotechnology Co., Ltd (Wuhan, China). Related antibodies, including TLR4, Pp65, p65, P-IκBα, IκBα, and Myd88 were purchased

from affinity biosciences (Jiangsu Qinke Biological Research Center Co., Ltd, Jiangsu, China). Lipopolysaccharide (LPS), monosaccharide standards were obtained from Sigma-Aldrich Co. (Beijing, China).

Extraction and purification of AKP

AKP was extracted by the method of dissolving in water and precipitating with ethanol. Briefly, areca nut kernel powder (50 g) was blended with 500 mL distilled water. The solution was extracted at 50 °C and 300 W for 1.5 h using an ultrasonic cleaning machine. Next, the suspension was centrifuged at 10,000 × g for 10 min, and the supernatant collected. The supernatant was then mixed with two volumes of 95% ethanol and stored at 4 °C for 12 h. Then centrifuged at 10,000 × g for 10 min, and the precipitate (crude AKP) collected. The crude AKP was then dissolved in water, then deproteinized using Sevage solution. The solution was then centrifuged, and the aqueous phase collected. The aqueous phase fraction was concentrated using a rotary evaporator. The deproteinized AKP was purified using a dialysis bag (8,000~14,000); deproteinized AKP was added into a dialysis bag and allowed to dialyze for 48 h in distilled water. At 4, 8, 14, 24, and 36 h of dialysis, the distilled water was replaced with fresh distilled water. Following dialysis, the polysaccharide solution was freeze-dried to obtain purified AKP.

Structural characterization of AKP

UV-vis determination

AKP (5 mg) was mixed with 1 mL of sterile water, and was completely dissolved by vortexing. The sample was analysed using a UV spectrometer (Agilent Cary 60), and a full-wavelength scan performed within the range of 200~1,000 nm, and a scanning interval of 1 nm.

Molecular weight determination

HPGPC-MALLS/RID (Agilent 1260 InfinityII MDS) was used for determining the molecular weight (M*w*) distribution and polydispersity (M*w*/M*n*) of AKP. AKP was dissolved in 0.1 M $NaNO_3$ until the final concentration reached 2 mg/mL, then filtered through a 0.45 μm membrane. Next, the filtrate (50 μL) was detected using PL aquagel OH mixed H column (8 μm, 7.5 mm × 300 mm, molecular weight range 200–10,000,000). Using differential and dual angle laser scattering detectors for detection, the flow rate was 1.0 mL/min, the column temperature was 45 °C. The mobile phase was 0.1 mol/L sodium nitrate with equal elution.

Monosaccharide composition determination

HPAEC-PAD (Agilent 1200) was used for determining the monosaccharide composition of the AKP. AKP (5 mg) was added into a hydrolysis tube with 1 mL of distilled water, and 1 mL of 4 mol/L trifluoroacetic acid, and nitrogen. For hydrolysis, the AKP was incubated at 110 °C for 5 h. Next, 0.1 mL of hydrolysis solution was transfered into a 4 mL PE tube, dried under vacuum at 50 °C for 2 h. Then 0.05 mL NaOH (0.3 mol/L) and 0.05 mL PMP methanol solution were added. The tube was filled with nitrogen and incubated at 70 °C for 1 h. Following incubation, 0.05 mL HCl (0.3 mol/L), 0.75 mL water, and 1.5 mL chloroform were added. The tube was shaken and then left to stand for layering. Once separate layers were observed, the lower layer of chloroform was discarded, the extraction was repeated three times. Finally, the water layer was filtered using a 0.45 μm filter. The filtrate (10 μL) was injected and analyzed using a C18 column (4.6 mm × 250 mm × 5 μm). The flow rate was 1.0 mL/min, the column temperature was 45 °C, detection wavelength was 254 nm with UV detectors. Mobile phase A was 0.1 mol/L 0.1 M KH_2PO_4 (pH 6.8), mobile phase B was acetonitrile, and the mobile phase gradient (A:B) was 82:18.

Scanning electron microscopy (SEM) analysis

AKP morphology was detected using scanning electron microscopy (TM4000, Japan). The AKP was sticked onto double-sided conductive tape, coated with gold and then observed. The acceleration potential was 15 kV.

X-ray (XRD) analysis

The crystalline structure of AKP was detected using an X-ray diffractometer (D/Max 2500 PC, Japan). Detection conditions used were as follows: radiation source, Cu and Kα, diffraction angle range 5° to 90° 2θ, step size 0.05°, 30 mA, 40 kV.

Fourier transform infrared (FTIR) spectroscopy analysis

The FTIR spectra of AKP was determined using a FTIR spectrometer (Thermo Fisher, USA). AKP (1.5 mg) and potassium bromide powder (150 mg) were vacuum compressed, then scanned within the wavenumber range of 400 to 4,000 cm^{-1}, each sample was scanned 64 times, with a resolution of 4 cm^{-1}.

Methylation analysis

The glycosyl linkages of AKP were detected using GC-MS (7890B-7000D, USA). AKP was methylated, hydrolyzed, reduced, and acetylated with CH_3I, trifluoroacetic acid, $NaBD_4$ and acetic anhydride respectively. Then filtered using a 0.45 μm membrane. The parameters of the chromatographic system were as follows: the detection volume was 1 μL, shunt ratio was 10:1, and the carrier gas was high purity helium. The initial temperature was 50 °C, maintained for 1.0 min, then 40 °C/min programmed to 215 °C, held for 45 min. The mass spectrometry system parameters were EI ion source, and the mass scan range was 30–600 m/z.

Nuclear magnetic resonance spectroscopy (NMR) analysis

AKP was dispersed in D_2O until the final concentration reached 40 mg/mL. Then the solution ws transferred to the NMR tube, and 1D and 2D NMR spectra were detected using a 500 MHz Nuclear Magnetic Resonance Spectrometer (Bruker, Germany).

Immunological activity analysis of AKP

Cell culture

Cell recovery: RAW264.7 macrophages were removed from liquid nitrogen and thawed in a 37 °C water bath, then transferred to a centrifuge tube containing 5 ml of medium. The RAW264.7 macrophages were obtained by centrifugation at 10,000 g for 10 min. The cell pellet was resuspended in complete culture medium containing fetal bovine serum, and inoculated into a culture dish for culture at 37 °C and 5% CO_2.

Cell passaging: The cells were passaged when the density of the cells reached 80% confluency. To dislodge wall-adherent cells from the bottom of the culture dish, a gentle blow was performed. The culture medium was collected by centrifugation at 10000 g for 10 min, and the supernatant discarded. The cell pellet wsa resuspended in PBS, centrifuged, and the supernatant discard. Finally, complete medium was added, a gentle blow was used to make a single-cell suspension, that was passed at a 1:3 ratio.

Cell grouping: RAW264.7 cells in the logarithmic growth phase with a density of 3.0×10^3 cells/well were inoculated into a 96-well plate and incubated at 37 °C in a humidified incubator with 5% CO_2 overnight. The experimental groups were as follows: (1) normal group; (2) LPS treatment group (1 μg/mL); (3) LPS treatment + polysaccharide treatment (20 μg/mL); (4) LPS treatment + polysaccharide treatment (40 μg/mL); (5) LPS treatment + polysaccharide treatment (80 μg/mL).

Cell viability assay

The viability of RAW264.7 cell was measured using a CCK-8 assay (Elabscience Biotechnology Co., Ltd). After incubation, 10 μl cck8 was added into each well, then incubated for 4 h at 37 °C. The OD values were determined at 450 nm using an enzyme labeling instrument.

Nitric oxide (NO) assay

After 24 h polysaccharide treatment, the NO content was detected using an NO content detection kit (Solarbio, Beijing, China).

Cytokine assay

The released content of interleukin-6 (IL-6), interleukin-1β (IL-1β), and tumor necrosis factor-α (TNF-α) were measured using ELISA kits (Solarbio, Beijing, China).

Western blot

The expression level of related proteins was determined referring to the method of Geng et al.[12]. Proteins were isolated from RAW264.7 cells using RIPA high-efficient lysate, and then transferred onto a PVDF membranes, then immersed in primary antibody incubation solution overnight. Then the thoroughly TBST-washed PVDF membrane was immersed in the secondary antibody incubation solution and soaked at 25 °C for 2 h. The enhancement solution in ECL (affinity) reagent was mixed with peroxidase solution, in a 1:1 ratio, and dropped on the PVDF membrane. Several minutes were allowed for reaction completion, then the excess substrate liquid was sucked off the membrane. After X-ray compression, the membrane was incubated in a developing solution and fixing solution. The membranes were then rinsed, dried, and scanned; ipp was used to analyze the film gray value. Related proteins, including TLR4, Pp65, p65, P-IκBα, IκBα, Myd88, and β-actin (1:1000 dilution for all) were included.

Statistical analysis

Excel was used to organize the data, the ANOVA module in SPSS 20.0 was employed for difference analysis, and Origin 2017 software was employed to draw graphs.

Results

Extraction, isolation, and Mw of AKP

The polysaccharide content of AN kernels was 14.8% (drybasis weight). Protein in the crude AN kernel polysaccharide was removed by using Sevage. Crude polysaccharide was further purified using a dialysis bag (8,000~14,000), and high purity polysaccharides from AN kernels were obtained after freeze-drying. The total sugar content of AKP was 88.36 ± 0.67 g/100 g, which meets the standard of subsequent analysis in structure and activity.

UV–vis spectroscopy (Fig. 1a) revealed that there was no absorption peak within the range of 260 to 280 nm, confirming that AKP components contained few nucleic acids and proteins[13].

The molecular weight (M*w*) can reflect the length of polysaccharide molecular chain, which may directly affected the bioactivity. The HPGPC-MALLS/RID chromatogram (Fig. 1b & c) shows that AKP had a single symmetrical and narrow peak, that can be considered a homogeneous polysaccharide[14]. The M*w* of the AKP was 6.95×10^5 Da. The polydispersity index was 1.35, which illustrated that the distribution of AKP molar mass was concentrated, which further illustrated that AKP was a relatively uniform polysaccharide.

Monosaccharide composition analysis

The monosaccharide composition of polysaccharide is closely related to the biological activity. As shown in Fig. 1d, the AKP was mainly composed of mannose (4.11×10^5 mg/kg), rhamnose (3.12×10^3 mg/kg), glucuronic acid (8.93×10^3 mg/kg), galacturonic acid (5.55×10^3 mg/kg), glucose (1.49×10^4 mg/kg), galactose (2.35×10^5 mg/kg), and arabinose (2.01×10^4 mg/kg). Mannose and galactose were the dominant monosaccharides, constituting 58.7% and 33.6% of AKP respectively. Indicating that AKP is a neutral polysaccharide, with a mannose and galactose backbone. This result coincided with the findings of Hu et al. and Ji et al.[10,15].

SEM analysis

SEM is mainly used to detected the microstructure on the surface of polysaccharides[14]. The surface morphology of AKP are shown in Fig. 2. The surface of AKP is smooth and has an irregular curly lamellar layer, indicating that there exists a strong attraction among the functional groups, forming the aggregation of molecule chains, and the aggregate appeared as an accumulation of crystals[16]. However, previous studies reported that the smooth surface of a polysaccharide may reduce its solubility[17].

XRD analysis

XRD technology was used to identify whether polysaccharides have crystal structures[18]. According to literature, crystalline structures exhibit sharp diffraction peaks, while amorphous structures exhibit broad peaks[19]. As shown in Fig. 3a, the XRD pattern of the AKP exhibited two small diffraction peaks between 10°–30°, indicating that the AKP interior contains both amorphous and crystalline structures.

FTIR analysis

The FTIR spectrum showed that the AKP has multiple characteristic absorption peaks in the of 4,000~400 cm^{-1} (Fig. 3b). The obvious peak at 3,600~3,200 cm^{-1} belonged to the O-H stretching vibration[20]. A strong peak at 2,922.79 cm^{-1} was ascribed to C-H asymmetric stretching vibrations[13]. The weak peak at 1,736 cm^{-1} represented the stretching vibration of C=O in the carboxyl groups, indicating the existence of uronic acids in the AKP, consistent with the monosaccharide composition. Peaks at 1,621.83 and 1,443.75 cm^{-1} were ascribed to the symmetric C=O stretching vibrations and asymmetric C=O stretching vibrations coupling C–H bending vibrations[21]. The peak at 1,383.96 cm^{-1} represented the bending vibration of C-H. The spectral bands that appeared in 1,200~1,000 cm^{-1} represented the stretching vibrations of functional groups C-O-H and C-O-C, the details are as follows: the significant peak at 1,074.51 cm^{-1} and 1,149.62 cm^{-1} indicated the presence of pyranose ring of sugar residues, and the absorption peak at 1,030 cm^{-1} was derived from the stretching variation of C-O-C group[13]. The peaks in the range of 1,000~800 cm^{-1} represented pyranose residue, the peak at 976 belonged to α-D glucopyranose, and three peaks at 872.94, 812.23, and 767 cm^{-1} confirmed the existence of α- and β-type glycosidic linkages in AKP[19]. In addition, some studies also pointed out that the peak at 765 cm^{-1} is the symmetric stretching vibrations of D-pyranose rings, and peaks at 872.94 and 812.23 cm^{-1} may indicate the presence of mannose residues, which is consistent with the findings of the present study where mannose is the main monosaccharide of the AKP. In general, the AKP structure consists of α- and β-type glycosidic bonds and D-pyranose rings. To obtain AKP structure information, further analysis, by methylation and NMR, was required.

Methylation analysis

Methylation analysis is commonly used to elucidate the glycosides bonding information of polysaccharides[13]. The connecting sites of the monosaccharide residues and the proportion of branch points and non-restore terminal unit information was identified using GC-MS. The total ion flow chromatogram and methylation mass spectrum of the AKP are shown in Fig. 4.

There were seven glycosidie bonds in the AKP (Table 1), including T-Ara*f*, T-Gal*p*, 4-Man*p*, 4-Glc*p*, 6-Gal*p*, 4,6-Man*p*, and 3,6-Gal*p*, and the relative molar ratios were 2.45, 39.50, 31.92, 1.65, 1.48, 21.95, and 1.05 respectively. Mannose and galactose residues were the main monosaccharide residues, which coincides with the analysis results of the monosaccharide composition, and T-linked galactose and 4-linked mannose residues were the major structural

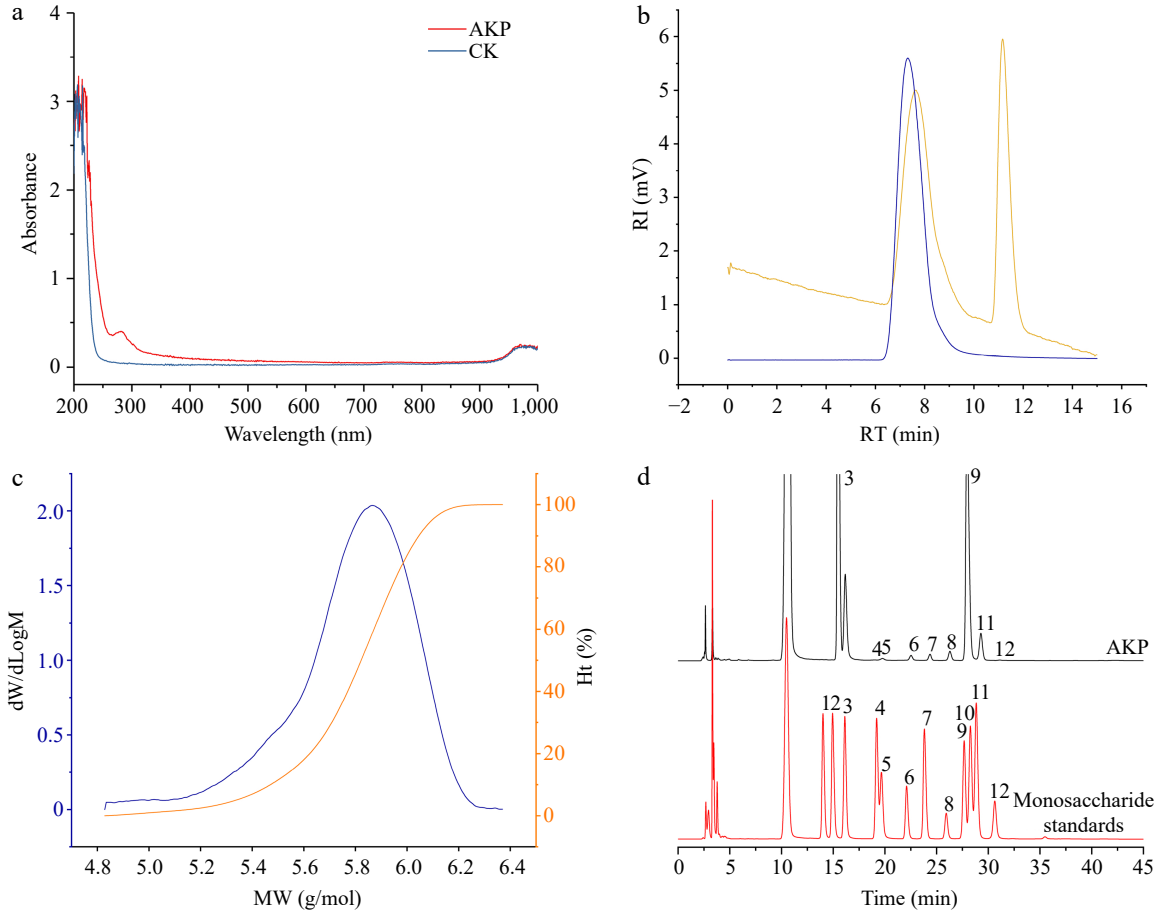

Fig. 1 (a) UV–Vis spectrum, (b) molecular weight chromatogram, (c) molecular weight distribution plot, and (d) monosaccharide composition of AKP. In (b), the blue line represents the dual angle laser light scattering signal, and the yellow line represents the differential signal. In (c) the blue line represents the molecular weight, and the orange line represents the proportion of molecular weight. In (d), the numbers were expressed as guluronic acid (1), mannuronic acid (2), mannose (3), ribose (4), rhamnose (5), glucuronic acid (6), galacturonic acid (7), glucose (8), galactose (9), xylose (10), arabinose (11), and fucose (12) respectively.

frameworks. In general, according to the methylation analysis, it is speculated that the main chain structure of AKP is composed of 4-linked Man*p* and 4,6-linked Man*p*, end of the terminal units Ara*f* and Gal*p*. In addition, the main and branch chains may also contain a small amount of 4-linked Glc*p*, 6-linked Gal*p*, and 3,6-linked Gal*p*.

NMR analysis

NMR is commonly used to detected the isomer of glycoside residues. The type, proportion, substitution site, and connection mode of monosaccharide residues in the sugar chain can be identified via the two- dimensional spectrum[22].

Heterohead hydrogen and heterohead carbon atom signals in one-dimensional NMR spectra are important for determining the information of polysaccharide residues. As reported in the literature, the polysaccharides signals in ^{1}H NMR were displayed at 3–6 ppm, of which δ 4.3–4.8 ppm was the heterohead hydrogen signal region of β-glycosidic bonding, δ 4.8–5.8 ppm was the heterohead hydrogen signal region of α-glycosidic bonding configuration[23]. The one-dimensional hydrogen spectra reveal that the AKP hydrogen spectral signals are mainly displayed at δ 3.0 and 5.5 ppm (Fig. 5a), indicating the existence of α-configuration and β-configuration glycosidic bonds in the structure of AKP, which is consistent with the results of the FTIR. Multiple coupling signal peaks were detected in the heterohead signal region at δ 4.3–5.8 ppm, indicating the presence of multiple sugar residues in the structure of the AKP, and the corresponding chemical shifts were δ 5.17, 4.95, and 4.43 ppm, respectively. The non-heteroheads of hydrogen signals were concentrated at δ 3.2–4.2 ppm, but the signals overlapping were serious, and it was necessary to combine the COSY and HSQC spectra to assign the chemical shifts of H2–H6 of each sugar residue.

As shown in Fig. 5b, the chemical shift signals of AKP in ^{13}C NMR were distributed more widely. The δ 95–110 ppm range was the C1 signal region of the sugar residues, of which δ 98–103 ppm was the heterocarbon signal region of the α-configuration and δ 103–106 ppm was the heterocarbon signal region of the β-configuration.

Multiple signal peaks were found in the heterocarbon region of AKP. To determine the assignment of the heteroclitic carbon signals, it is necessary to conduct an analysis by combining ^{13}C NMR and HSQC spectra. The heterocapitated carbon signals δ 98.77 ppm, δ 103.13 ppm, δ 103.15 ppm, and δ 109.28 ppm in the δ 95–110 ppm range of the carbon spectrum corresponded to the end-group proton signals δ 4.95 ppm, δ 4.43 ppm, δ 4.43 ppm, and δ 5.17 ppm in the hydrogen spectrum, which were marked as glycoconjugate residues A, B, C, and D respectively. The H1 and CI chemical shifts were δ 4.95 ppm and δ 98.77 ppm for sugar residue A, δ 4.43 ppm and δ 103.13 ppm for sugar residue B, δ 4.43 ppm and δ 103.15 ppm for sugar residue C, and δ 5.17 ppm and δ 109.28 ppm for sugar residue D. Combined with the methylation information, and heterohead signal, it was hypothesized that sugar residue A was α-D-Gal*p*-(1→, residue B was →4)-β-D-Man*p*-(1→, residue C was →4,6)-β-D-Man*p*-(1→, and residue D was α-L-Ara*f*-(1→.

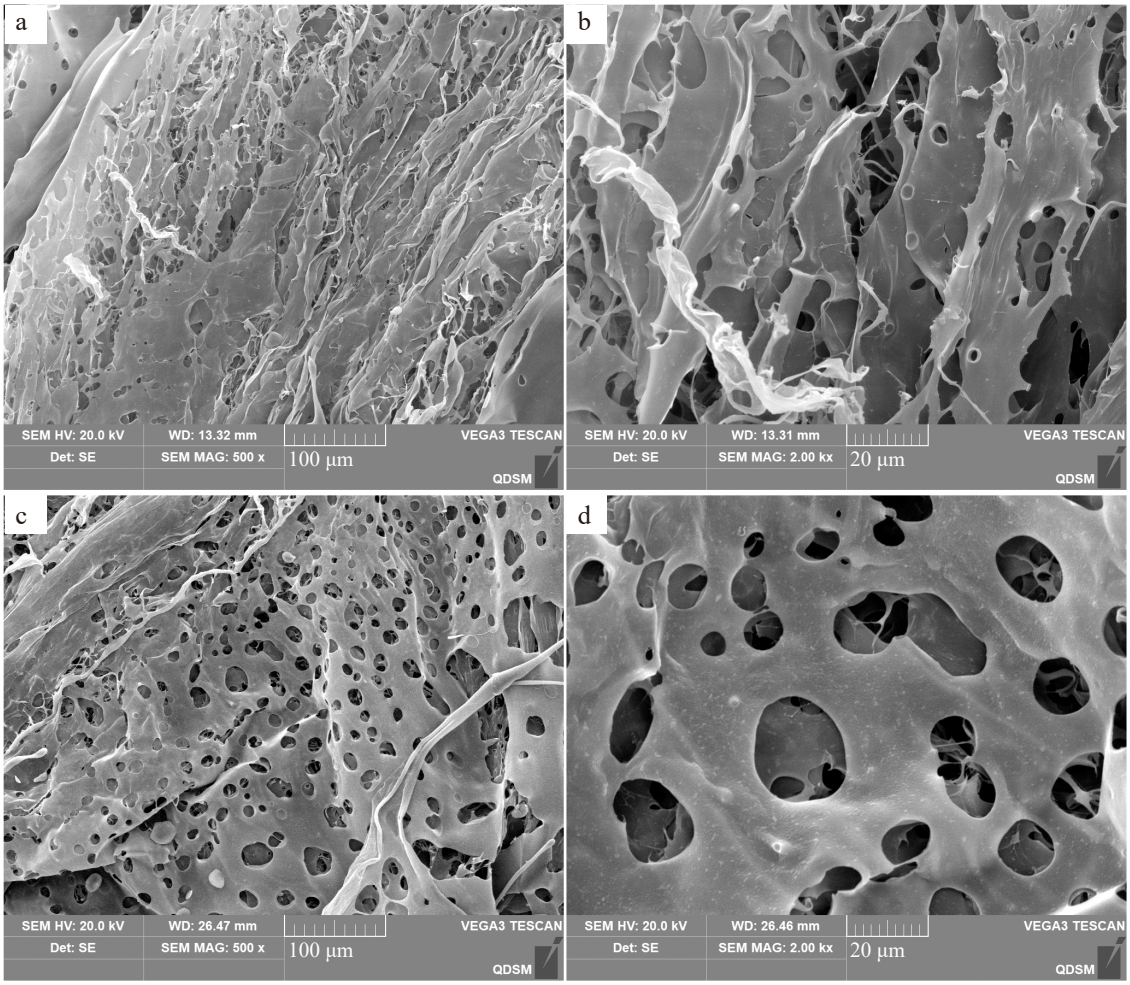

Fig. 2 The microstructure of AKP at different positions. (a), (c) magnification 500×; (b), (d) magnification 2,000×.

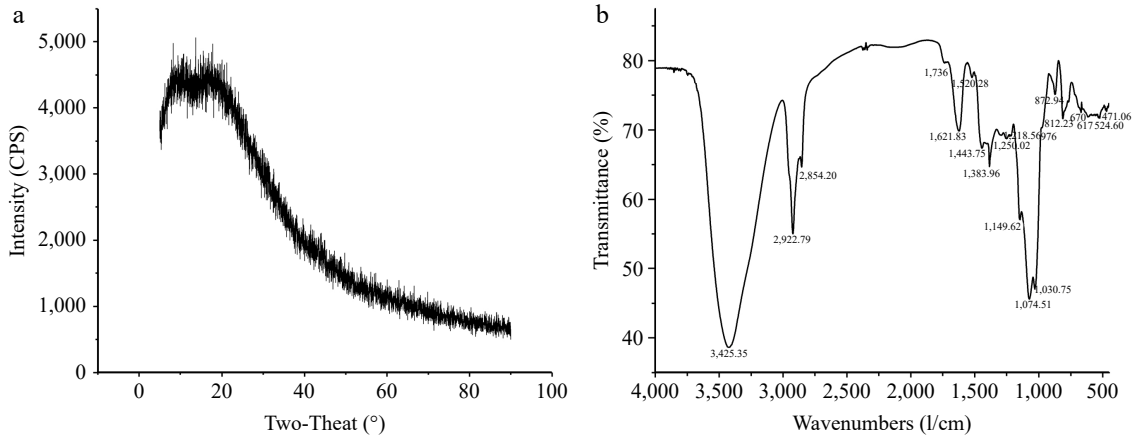

Fig. 3 (a) X-ray diffraction pattern, and (b) FTIR spectrum of AKP.

The COSY spectrum (Fig. 5c) responds to the adjacent proton hydrogen correlation signals in the sugar residues, the HSQC spectrum (Fig. 5e) reflects the correlation signals of directly connected carbons and hydrocarbons[24]. Based on the H1 and C1 chemical shifts of sugar residues A, B, C, and D, the chemical shifts of individual sugar residues were attributed in combination with COSY and HSQC spectrum, and the results are shown in Table 2.

According to the chemical shifts of each sugar residue, HMBC and NOESY spectra were combined to analyzed the structure and linkage mode of each residue in AKP (Fig. 5d, f). Since the sugar residues signals in the HMBC spectra were weak, it was difficult to recognize and characterize the residues. Therefore, the connection order of each sugar residue in AKP was inferred mainly based on the NOESY spectrum. The cross peaks of A-H1 and C-H6 appeared at δ 4.95/3.74 ppm, the cross peaks of B-H1 and C-H4 appeared at δ 4.43/3.87 ppm, and the cross peaks of C-H1 and B-H4 showed up at δ 4.43/3.86 ppm. The cross peaks of D and other sugar residues were not recognized. This might be associated with the low content of the sugar residue D.

According to the NMR information, it was deduced that the main chains of the AKP is →4)-β-D-Man*p*-(1→, and the branched chains

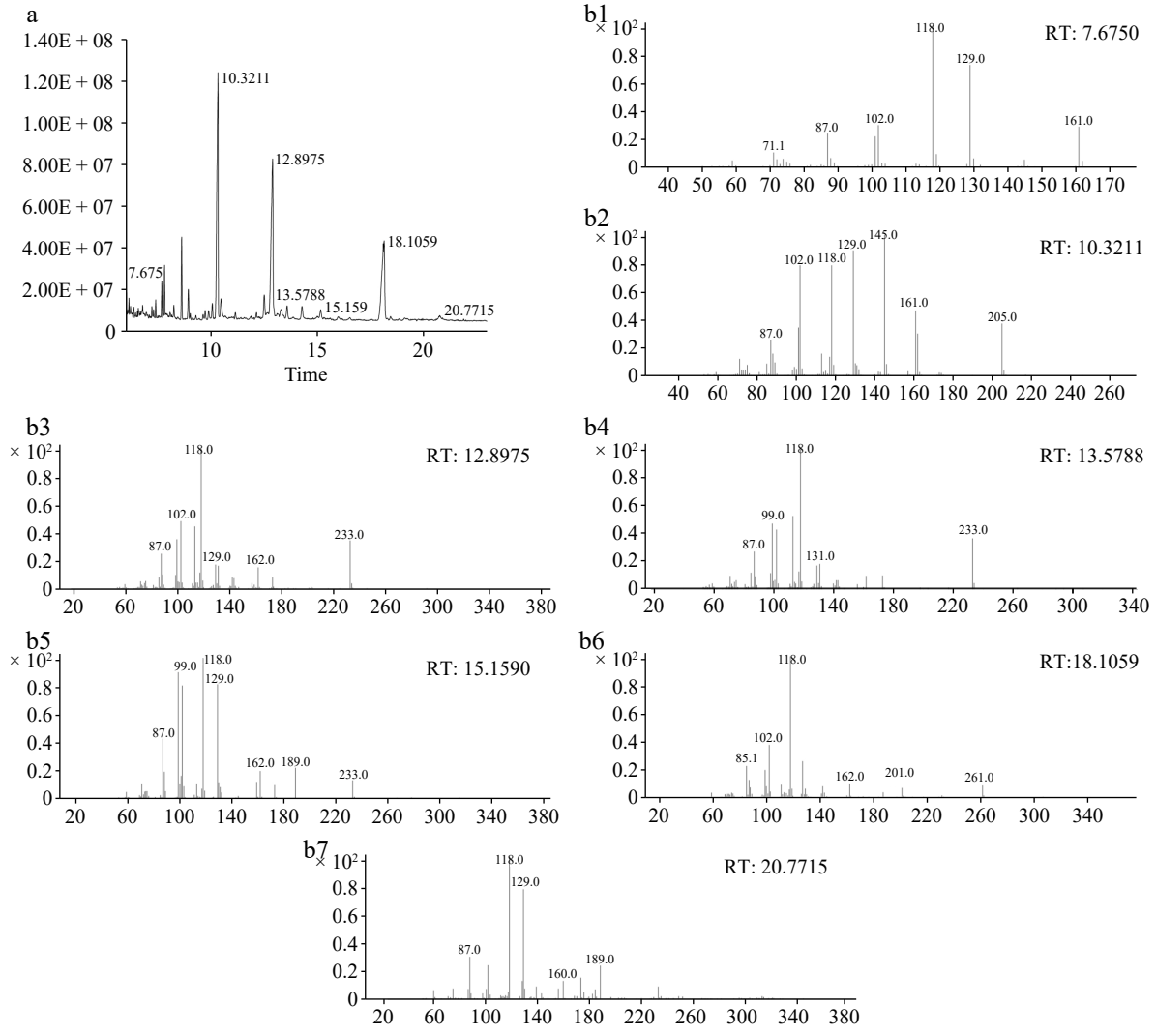

Fig. 4 (a) The total ion flow chromatogram, and (b) methylation mass spectrum of AKP. (b1)–(b7) Represent T-Araf, T-Galp, 4-Manp, 4-Glcp, 6-Galp, 4,6-Manp, and 3,6-Galp respectively.

Table 1. AKP methylation analysis data.

Linkage type	Retention time (min)	Derivative name	MW	Relative molar ratio (%)
T-Ara*f*	7.675	1,4-Di-O-acetyl-1-deuterio-2,3,5-tri-O-methyl-D-arabinitol	279	2.45
T-Gal*p*	10.3211	1,5-Di-O-acetyl-1-deuterio-2,3,4,6-tetra-O-methyl-D-galactitol	323	39.50
4-Man*p*	12.8975	1,4,5-Tri-O-acetyl-1-deuterio-2,3,6-tri-O-methyl-D-mannitol	351	31.91
4-Glc*p*	13.5788	1,4,5-Tri-O-acetyl-1-deuterio-2,3,6-tri-O-methyl-D-glucitol	351	1.64
6-Gal*p*	15.159	1,5,6-Tri-O-acetyl-1-deuterio-2,3,4-tri-O-methyl-D-galactitol	351	1.47
4,6-Man*p*	18.1059	1,4,5,6-Tetra-O-acetyl-1-deuterio-2,3-di-O-methyl-D-mannitol	379	21.95
3,6-Gal*p*	20.7715	1,3,5,6-tetra-O-acetyl-2,4-di-O-methyl galactitol	379	1.05

were mainly composed of α-D-Gal*p*-(1→ attached to the O-6 position of →4,6)-β-D-Man*p*-(1→. Therefore, it is hypothesized that the repeating unit of the polysaccharide chain may be:

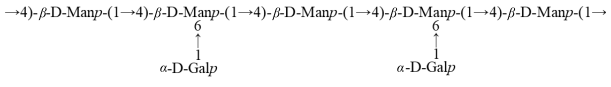

Immunomodulatory activity of AKP

Effect of AKP on cell viability

In order to determine the optimal culture time for RAW264.7 macrophage and the optimal concentration of AKP, this study compared the effects of different concentrations of AKP (1.25, 2.5, 5, 10, 20, 40, 80, 160, 320, and 640 μg/mL), at different treatment times (12, 24, 48, and 72 h), on RAW264.7 macrophages viability. Results are shown in Fig. 6.

At treatment times of 12, 24, 48, and 72 h, the viability of RAW264.7 macrophages exhibited an ascending trend with the increasing concentration of AKP (in the concentration range of 1.25–40 μg/mL), indicating that AKP showed no cytotoxicity of RAW264.7 macrophages at concentration of 1.25–40 μg/mL. Under the action time of 12 and 24 h, the cell viability was the highest at AKP = 40 μg/mL. At 48 h, the cell viability was highest at AKP = 20 μg/mL, whereas at 72 h, the cell viability was highest at AKP = 10 μg/mL. As the acting concentration of AKP continued to increase,

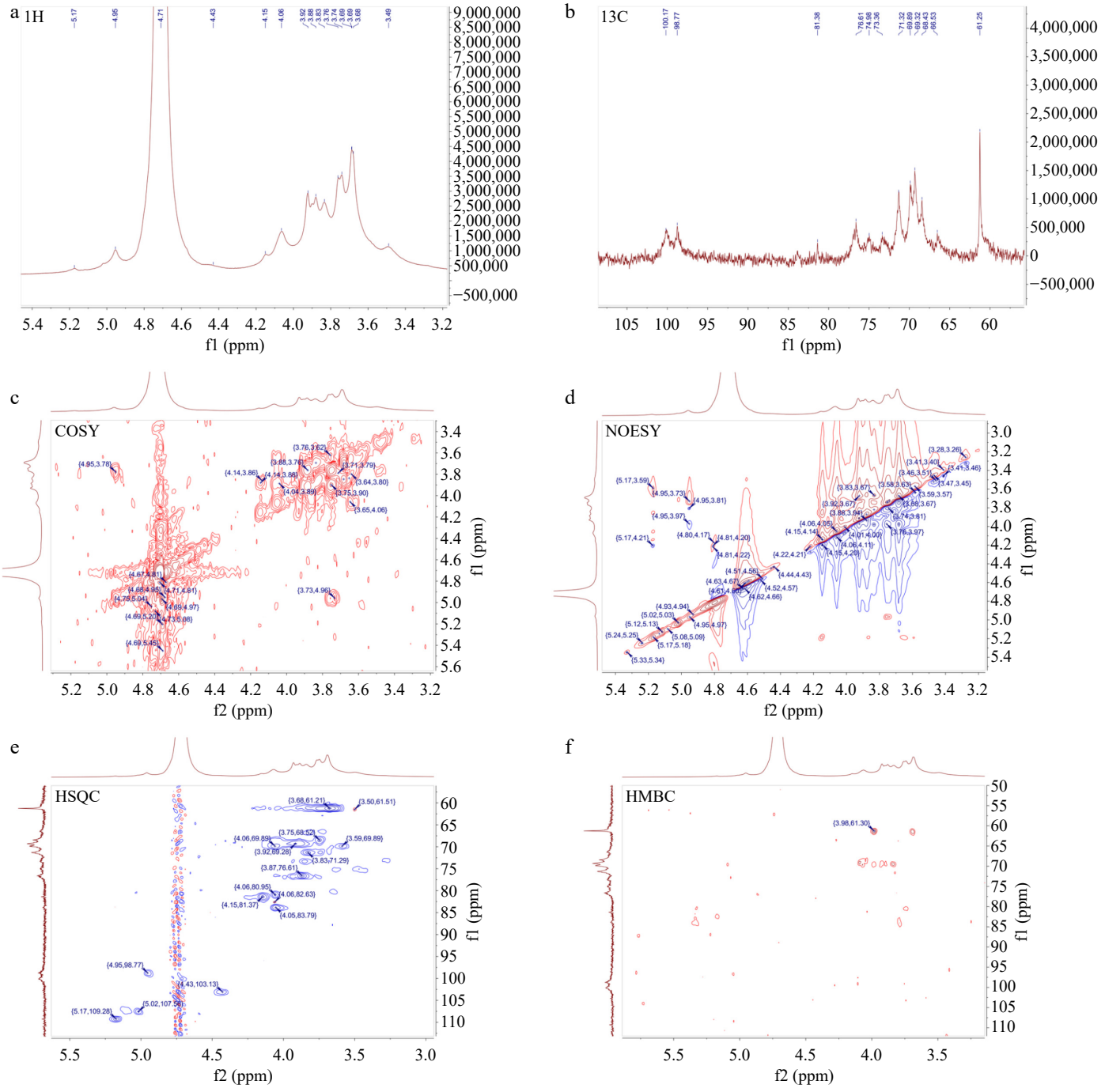

Fig. 5 One-dimensional and two-dimensional nuclear magnetic resonance spectrum of AKP. (a) ^{1}H NMR spectrum, (b) ^{13}C NMR spectrum, (c) COSY spectrum, (d) NOESY spectrum, (e) HSQC spectrum, (f) HMBC spectrum.

the viability of macrophages decreased, in a dose-dependent manner, and is statistically significant ($p < 0.01$). To visualize the effect of AKP concentration on the cells at a later stage, the AKP concentrations of 20, 40, and 80 μg/mL were selected for the next experiments.

Effect of AKP on the viability and phagocytic activity

To investigate the effect of AKP on the proliferation and phagocytosis of inflammatory cells, RAW264.7 macrophages were treated with LPS for the establishment of an inflammatory cell model. Subsequently, AKP acted with LPS-induced macrophages to observe cell viability and phagocytosis, the results are shown in Fig. 7a & b.

LPS significantly reduced the viability of cells ($p < 0.05$) when compared with the control group, while AKP significantly increased the viability of inflammatory cells models at concentrations of 20, 40, and 80 μg/mL, indicating that AKP could stimulate RAW264.7 macrophage growth.

The first step for macrophages to exert an immune effect is to exert phagocytosis[20]. The phagocytic activity of the LPS-induced cells was significantly increased and was twice that of the normal cells, indicating that LPS-induced macrophages exerts a severe inflammatory response, and an excessive systemic inflammatory response can lead to tissue damage. AKP intervention significantly reduced the phagocytic activity of LPS-induced cells, in a

Table 2. Chemical shifts of sugar residues ^{1}H and ^{13}C.

Code	Glycosyl residues	Chemical shifts (ppm)					
		H1/C1	H2/C2	H3/C3	H4/C4	H5/C5	H6/C6
A	α-D-Gal*p*-(1→	4.95	3.77	3.74	4.06	3.84	3.69
		98.77	71.33	71.21	69.89	73.34	61.21
B	→4)-β-D-Man*p*-(1→	4.43	3.6	3.83	3.86	3.88	3.84,3.5
		103.13	69.78	71.33	76.65	69.22	61.35
C	→4,6)-β-D-Man*p*-(1→	4.43	3.59	3.83	3.87	n.d.	3.74,4.07
		103.15	69.87	71.2	76.65	n.d.	68.41
D	α-L-Ara*f*-(1→	5.17	4.15	n.d.	4.05	n.d.	/
		109.28	81.37	n.d.	83.79	n.d.	/

n.d.: not detected.

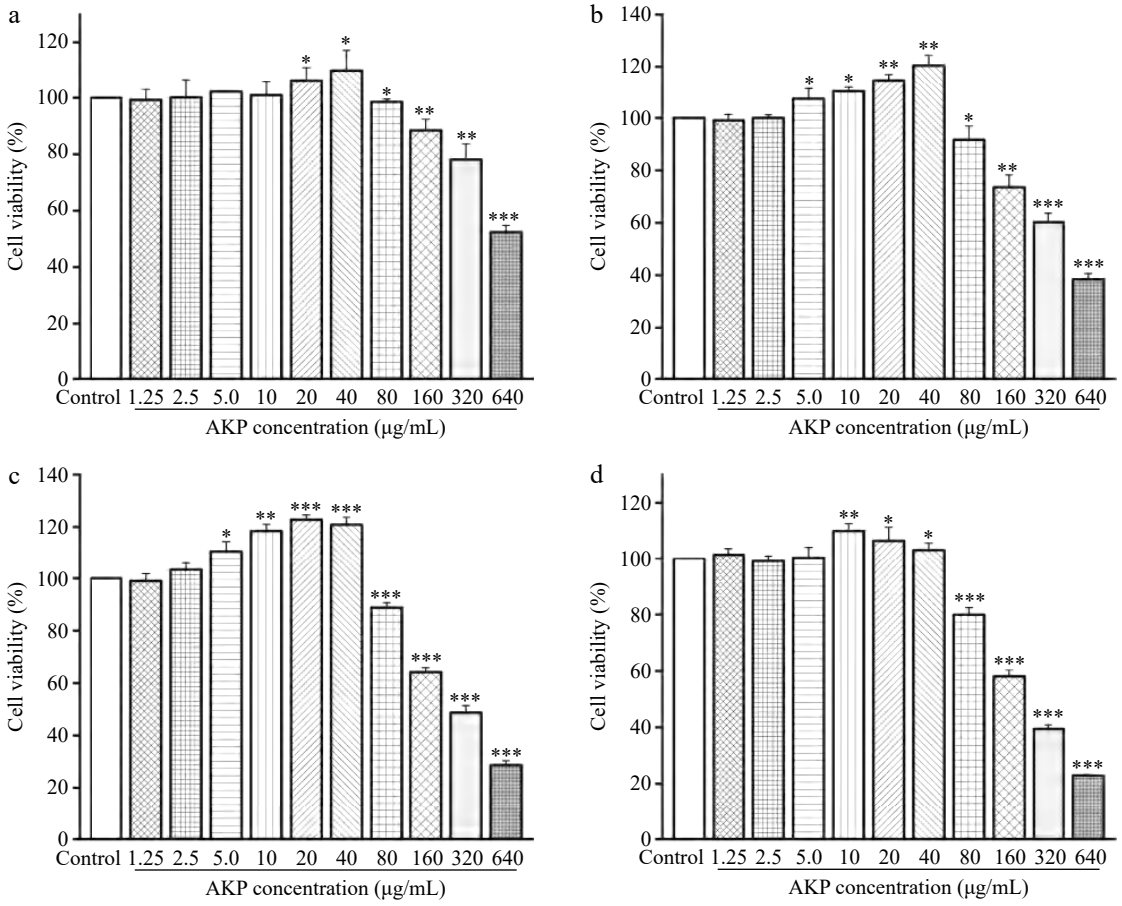

Fig. 6 Effect of AKP concentration and treatment time on the cell viability. Compared with the control group, *** $p < 0.001$, ** $p < 0.01$, * $p < 0.05$. (a)–(d) represent the treatment time of 12, 24, 48, and 72 h, respectively

dose-dependent manner. Besides, phagocytic activity at AKP = 80 μg/mL was still greater than that of the normal cells. From the perspective of phagocytic activity, AKP significantly inhibits LPS-induced macrophage phagocytosis and exhibits a strong immune regulatory effect.

Effect of AKP on the NO production

NO can promote the activation of macrophages and the release of related inflammatory factors, and then regulate the process of immune responses. At the same time, NO also has certain cytotoxic effects[25].

Compared with the normal control group, the NO production of cells increased significantly ($p < 0.001$) following LPS induction (Fig. 7c). These findings indicate that LPS treatment induces RAW264.7 macrophages, triggers a strong immune response, and release a large amount of NO. Compared with the LPS-induced group, intervention with different concentrations of AKP significantly reduced NO release in inflammatory cells ($p < 0.01$), and exhibiting an inhibitory effect on LPS-induced NO elevation in a dose-dependent manner. Indicating that the response triggered by AKP was milder than that induced by LPS, suppresses the excessive production of NO and reducing the harm of excessive NO to the human body. Notably, the NO release of RAW264.7 cells at the AKP level of 80 μg/mL was lower than that at the concentrations of 20 and 40 μg/mL, indicating that low concentrations of AKP can activate RAW264.7 cells, promote the release of large amounts of NO, and produce immune effects, while high concentrations of AKP may have a feedback regulatory effect on cellular activation and inhibit the uncontrolled inflammatory effects of cells due to constant NO secretion. Overall, AKP exhibited strong immunomodulatory activity, from the perspective of NO release.

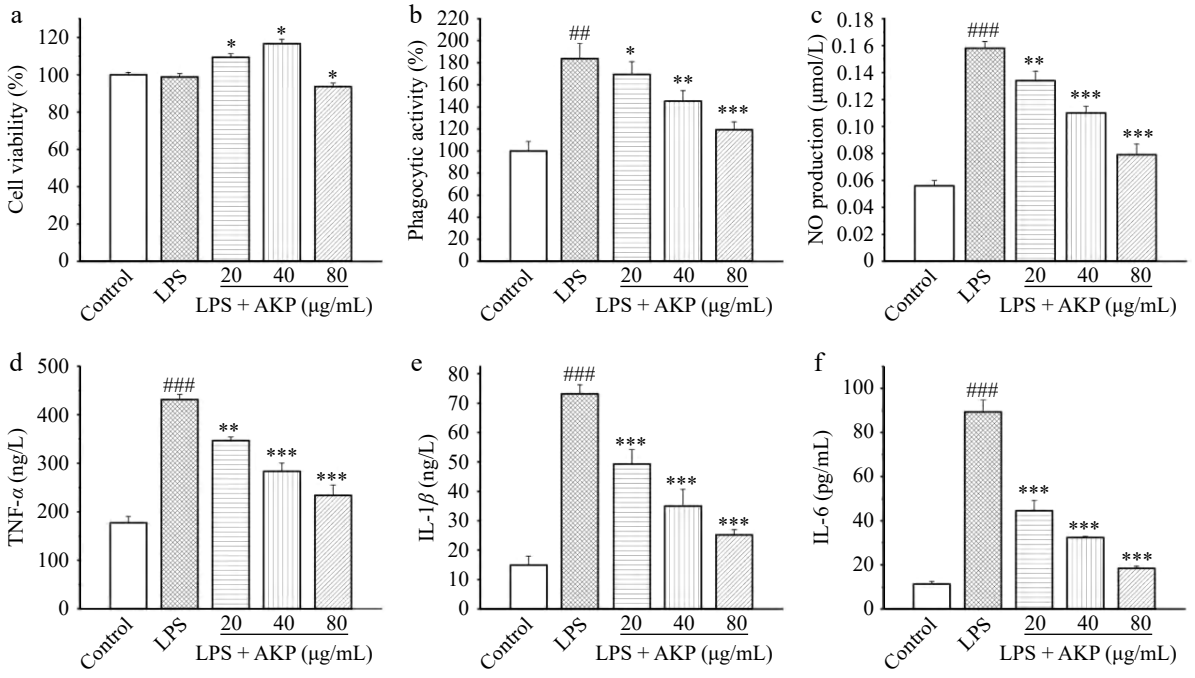

Fig. 7 Effect of AKP on the (a) cell viability, (b) phagocytic activity, (c) NO production, (d) IL-1β release, (e) IL-6 release, and (f) TNF-α release of LPS-induced RAW264.7 cells. Compared with the control group, ### $p < 0.001$; Compared with the model group, *** $p < 0.001$, ** $p < 0.01$, * $p < 0.05$.

Effect of AKP on the cytokine levels

Polysaccharides exhibit biological activity through activating the immune function of macrophages[26]. Once polysaccharides bind to receptors on the surface of macrophages, macrophages will be triggered and then generate a large quantity of cytokines, such as tumor necrosis factor TNF-α, and interleukin[20].

LPS enhanced the secretion of TNF-α (Fig. 7d), IL-1β (Fig. 7e), and IL-6 (Fig. 7f) in inflammatory cells ($p < 0.001$), reaching the highest levels of 431.2 ng/L, 73.1 ng/L, and 89.3 pg/mL respectively, which was 2.4-fold, 4.9-fold, and 7.9-fold that of normal cells. By contrast, the production of TNF-α, IL-1β, and IL-6 in inflammatory cells decreased significantly after AKP treatment ($p < 0.001$, $p < 0.01$), and the degree of reduction was positively correlated with the concentration of AKP. The level of TNF-α, IL-1β, and IL-6 stimulated by AKP at concentration 80 μg/mL reached the lowest values of 233.7 ng/L, 25.2 ng/L, and 18.5 pg/mL, and the inhibition rates were 45.7%, 65.5%, and 79.3% respectively. The production of inflammatory cytokines can lead to various validation cascade reactions, stimulating cells to continuously release inflammatory factors, exacerbating inflammation and leading to an inflammatory storm, damaging the immune system. AKP significantly decreased the production of TNF-α, IL-6, and IL-1β in LPS-induced inflammatory cells, indicating that AKP can inhibit the over release of pro-inflammatory factors induced by LPS, enabling the body to better exert its immune function.

Effect of AKP on the TLR4/NF-κB signaling pathway related proteins

Based on the previous research findings, AKP showed strong immunomodulatory activity. To further explore the possible reason by which AKP exerts its immune effects, the changes in the levels of related proteins in the TLR4/NF-κB pathways were analyzed by using western blot analysis.

As shown in Fig. 8, LPS significantly enhanced the TLR4, P65, IκB-α, and MyD88 protein in macrophages ($p < 0.05$, $p < 0.01$, $p < 0.001$), while AKP treatment significantly decreased the levels of these protein, and show a dose-dependent relationship. This result indicates that AKP attenuates LPS-induced inflammation in RAW264.7 macrophages by decreasing the level of TLR4, P65, Pp65, IκB-α, and MyD88 in the TLR4/NF-κB signaling pathway.

Disscussion

The structural of AKP

The chemical structure of polysaccharides is highly relevant to their sources[15]. In addition, polysaccharide fractions within the same sample have different structures, and these structures are closely associated with their biological activity[27,28].

According to the present results, AKP was a relatively homogeneous polysaccharide. The M*w* was 6.95 × 10^5 Da. While Ji et al. reported the M*w* of a neutral polysaccharide from Areca nut was 3.73 × 10^4 Da, which is lower than that of the AKP isolated in the present study[15]. The research results of Hu et al. showed that the M*w* range of Areca nut seeds polysaccharide was 1.84 × 10^4 to 4.79 × 10^5 g/mol[10]. The difference between the M*w* may be related to the sample source, the experimental method of isolation and the detection method. According to the analysis of structural characterization, the main chain of AKP is →4)-β-D-Man*p*-(1→, and the branched chain is α-D-Gal*p*-(1→ attached to the O -6 position of →4,6)-β-D-Man*p*-(1→. Mannose and galactose residues were the main monosaccharide residues, consistent with the results of monosaccharide composition analysis. The connecting of monosaccharide residues and the presence of repeating units indicatied strong attraction and aggregation of polysaccharide chains, which also leads to the existence of crystalline regions and in AKP. Thus the XRD pattern of AKP exhibited two small diffraction peaks between 10–30°, and the surface of AKP is smooth and has an irregular curly lamellar layer.

Immune regulation mechanism analysis

The TOLL-like receptor family is the major transmembrane receptor family of pattern recognition receptors, of which TLR4 is an important receptor for natural product polysaccharides and is expressed in a wide range of immune cells, mediating the

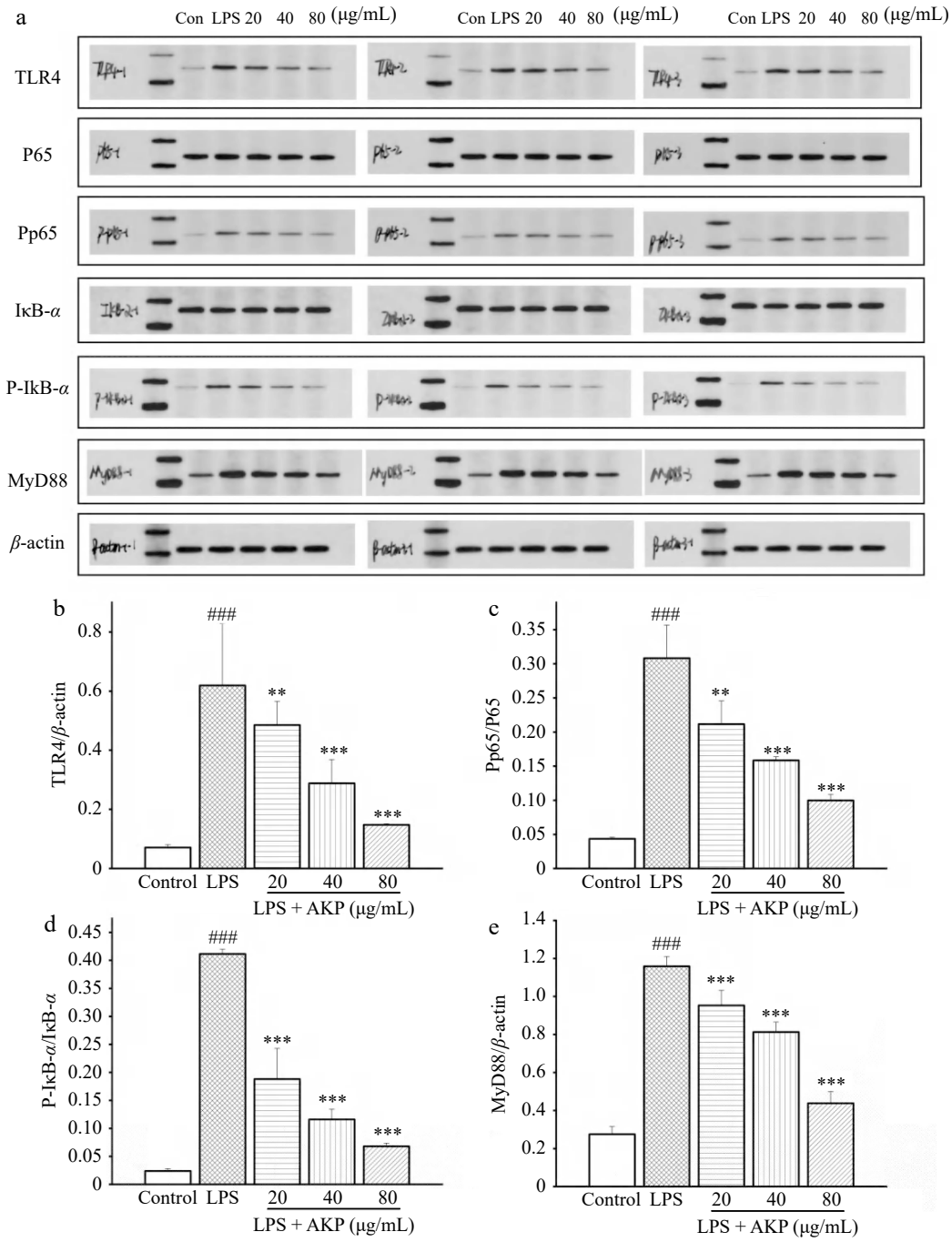

Fig. 8 Effect of AKP on the TLR4/NF-kB signaling pathway related proteins in RAW264.7 cells induced by LPS. (a) Protein imprinting map, (b) TRL4 protein expression, (c) P-P65/P65 protein expression, (d) P-IκB-α/IκB-α protein expression, (e) MyD88 protein expression. Compared with control group, ### $p < 0.001$; Compared with model group, *** $p < 0.001$, ** $p < 0.01$. Three columns represent three repeated experiments.

immunomodulatory effects of a wide range of phytopolysaccharides[29]. LPS is an inducer of innate immune responses, and TLR4 is a key receptor mediating the activation of inflammatory cascade responses by LPS[30]. In the early stages of infection, LPS-induced TLR4 activation and cytokine production are beneficial to the organism in the early stages of infection, but when this process is out of control, over-activation of TLR4 by LPS can lead to cytotoxicity, infectious shock, and in severe cases, death.

LPS binds to the TLR4 receptor macrophages, upregulates TLR4 protein expression, activates the downstream MyD88-dependent signaling pathway to transmit inflammatory signals, and further activates NF-κB, which is participated in regulating DNA transcription, apoptosis, cytokine release, and activation of the immune response[31]. In the absence of NF-κB activation, p65 is a subunit component of NF-κB that binds to its inhibitory protein IκB-α in the cytoplasm. When an external signal binds to a receptor of the cell membrane, the receptor conformation changes, transmits the signal and activates IκB-α kinase phosphorylation, ubiquitination, and detachment from NF-κB, resulting in the release and activation of NF-κB in the cytoplasm[32]. The activated NF-κB binds to relevant DNA after entering the nucleus, promoting the production of inflammatory factors (TNF-α, IL-6, and IL-1β), exacerbating the inflammatory response, and severely damaging cellular tissue. This study showed that in the LPS-induced model cells, TLR4, P65, IκB-α,

and MyD88 expression increased significantly, suggesting that the nuclear translocation of P65 and the downstream inflammatory pathway were activated in RAW264.7 macrophages, and the expression of cytokines TNF-α, IL-1β, and IL-6 increased, exacerbating cellular inflammation. In contrast, AKP significantly inhibited the expression of TLR4, MyD88, IκB-α, and P65 proteins induced by LPS: AKP not only inhibited the nuclear translocation of P65 and the excessive activation of the downstream NF-κB inflammatory pathway, but also reduced the release of downstream inflammatory factors (IL-6, IL-1β, and TNF-α). Thus, AKP can inhibit inflammatory responses and exert ameliorative effects through the regulation of the TLR4/NF-κB signaling pathway. Nevertheless, the specific sites where AKP exerts its anti-inflammatory effects and the more profound mechanism of action require further research for elucidation.

Structure-immunomodulation relationship analysis

Based on the present results, AKP exhibits strong immunomodulatory activity *via* TLR4/NF-κB signaling pathway regulation, inhibiting the release of TNF-α, IL-6, and IL-1β. Macrophage activation of polysaccharides are influenced by their structural features, including M*w*, type of monosaccharide, branch degree, and so on[33]. The molecular weight of polysaccharides affects TLR4-binding, and polysaccharides with a M*w* between 10 and 1,000 kDa dramatically stimulate macrophages and bind to TLR4[12,21]. In the present study, it was found that the M*w* of AKP was 6.95×10^5 Da. Consistently, AKP exhibited immunomodulatory activity by stimulating the TLR4/NF-κB signaling pathway. The presence of monosaccharides like Gal, Glc, Man, and Rha had a powerful impact on the immune response through TLR4-binding[12]. AKP exhibited a rich monosaccharide composition that included: mannose, galactose, galacturonic acid, glucuronic acid, and glucose. In addition, polysaccharides with a high uronic acid content exerts strong immunomodulatory activity[34]. The content of galacturonic acid and glucuronic acid was 5.55×10^3 and 8.93×10^3 mg/kg, respectively, which may have contributed to the strong immunoregulatory effects exerted by AKP. As mentioned above, the glycosidic linkages also significantly affect the immunomodulatory activity of polysaccharide; β-D-glucan is one of the active ingredients that exhibit biological activity, β-1-6 linked glucose confers strong immunomodulatory activity, and polysaccharides with multiple types of glycosidic bonds have stronger immune regulatory functions[26]. Since AKP is rich in different glycosidic bond types and contains β-D-Man*p* in the main chain, this may have contributed to the high immunoreactivity of AKP.

Conclusions

A homogeneous polysaccharide AKP was isolated from the kernels of Areca nut. Chemical structure analysis demonstrated that the average M*w* of AKP was 6.95×10^5 Da. Mannose (58.7%) and galactose (33.6%) were the dominant AKP monosaccharides. Methylation and NMR analyses suggest that the main chain of AKP was →4)-β-D-Man*p*-(1→, and the branched chain was α-D-Gal*p*-(1→ attached to the O-6 position of →4,6)-β-D-Man*p*-(1→. Furthermore, the immunostimulatory activity of AKP was evaluated by RAW264.7 macrophage inflammation model induced by LPS; it was found that AKP attenuates inflammation *via* TLR4/NF-κB pathway regulation by decreasing TLR4, P65, IκB-α, MyD88, and inhibiting the production of NO, TNF-α, IL-6, and IL-1β. The strong immune activity exerted by AKP is attributed to its diverse monosaccharide, high Mw, and the existence of β-D-Man*p* in the main chain. These findings offer a theoretical basis and reference for the broad clinical application of AKP for the treatment of numerous diseases.

Author contributions

The authors confirm contribution to the paper as follows: study conception and design, Feng X, Zhang J, Dai J, Wang S, Kang X, Ji J, Dai W; data collection: Zhang J, Dai J, Rui K; analysis and interpretation of results: Zhang J; draft manuscript preparation: Zhang J, Feng X; Manuscript revision: Zhang J, Feng X. All authors reviewed the results and approved the final version of the manuscript.

Data availability

Data sharing not applicable to this article as no datasets were generated or analyzed during the current study.

Acknowledgments

This work was supported by the Project of Sanya Yazhou Bay Science and Technology City (Grant No. SC-YRC-2022-103), the Natural Science Foundation of Hainan (Grant No. 321QN356), and the Talent Start-up Funding of Hainan Academy of Agricultural Sciences (Grant No. HAAS2023RCQD07).

Conflict of interest

The authors declare that they have no conflict of interest.

Dates

Received 6 August 2024; Revised 25 November 2024; Accepted 5 December 2024; Published online 22 May 2025

References

1. Peng W, Liu YJ, Wu N, Sun T, He XY, et al. 2015. *Areca catechu* L. (Arecaceae): a review of its traditional uses, botany, phytochemistry, pharmacology and toxicology. *Journal of Ethnopharmacology* 164:340–56
2. Oliveira NG, Ramos DL, Dinis-Oliveira RJ. 2021. Genetic toxicology and toxicokinetics of arecoline and related areca nut compounds: an updated review. *Archives of Toxicology* 95:375–93
3. Liu YJ, Peng W, Hu MB, Xu M, Wu CJ. 2016. The pharmacology, toxicology and potential applications of arecoline: a review. *Pharmaceutical Biology* 54:2753–2760
4. Mei F, Meng K, Gu Z, Yun Y, Zhang W, et al. 2021. Arecanut (*Areca catechu* L.) seed polyphenol-ameliorated osteoporosis by altering gut microbiome via LYZ and the immune system in estrogen-deficient rats. *Journal of Agricultural and Food Chemistry* 69:246–58
5. Ji XL, Guo JH, Tian JY, Ma K, Liu YQ. 2023. Research progress on degradation methods and product properties of plant polysaccharides. *Journal of Light Industry* 38(3):55–62
6. Yu Y, Shen M, Song Q, Xie J. 2018. Biological activities and pharmaceutical applications of polysaccharide from natural resources: a review. *Carbohydrate Polymers* 183:91–101
7. Tang MM, Song F, Wang H, Zhao SL, Chen WJ. 2015. *In vitro* antioxidant activities and protective effects of polysaccharides from *Areca catechu* L. *seed. Chinese Journal of Tropical Crops* 36:1136–41
8. Yin MS, Ding HH, Pan FB, Kuang FJ, Ji XL, et al. 2021. Optimization of ultrasonic-assisted aqueous awo-phase extraction of *Areca catechu* L. polysaccharide using response surface design and assessment of its antioxidant activities. *Food Research and Development* 42(19):163–70
9. Tang MM, Chen H, Li R. 2019. Optimization of ultrasound-assisted extraction of areca nut polysaccharides based on response surface methodology and anti-inflammatory activity. *Anhui Agricultural Science Bulletin* 25:21–24,74
10. Hu M, Peng W, Liu Y, Wu N, Zhao C, et al. 2017. Optimum extraction of polysaccharide from areca catechu using response surface

methodology and its antioxidant activity. *Journal of Food Processing and Preservation* 41:e12798

11. Ji X, Guo J, Pan F, Kuang F, Chen H, et al. 2022. Structural elucidation and antioxidant activities of a neutral polysaccharide from arecanut (*Areca catechu* L.). *Frontiers in Nutrition* 9:853115
12. Geng L, Zhang Q, Li Q, Zhang Q, Wang C, et al. 2024. Fucoidan from the cell wall of Silvetia siliquosa with immunomodulatory effect on RAW 264.7 cells. *Carbohydrate Polymers* 332:121883
13. Li L, Qiu Z, Dong H, Ma C, Qiao Y, et al. 2021. Structural characterization and antioxidant activities of one neutral polysaccharide and three acid polysaccharides from the roots of *Arctium lappa* L.: a comparison. *International Journal of Biological Macromolecules* 182:187–196
14. Ji X, Cheng Y, Tian J, Zhang S, Jing Y, et al. 2021. Structural characterization of polysaccharide from jujube (*Ziziphus jujuba* Mill.) fruit. *Chemical and Biological Technologies in Agriculture* 8:54
15. Ji X, Peng Q, Yuan Y, Shen J, Xie X, et al. 2017. Isolation, structures and bioactivities of the polysaccharides from jujube fruit (*Ziziphus jujuba* Mill.): a review. *Food Chemistry* 227:349–357
16. Wang L, Zhao Z, Zhao H, Liu M, Lin C, et al. 2022. Pectin polysaccharide from *Flos Magnoliae* (Xin Yi, *Magnolia biondii* Pamp. flower buds): Hot-compressed water extraction, purification and partial structural characterization. *Food Hydrocolloids* 122:107061
17. Chen Z, Zhao Y, Zhang M, Yang X, Yue P, et al. 2020. Structural characterization and antioxidant activity of a new polysaccharide from *Bletilla striata* fibrous roots. *Carbohydrate Polymers* 227:115362
18. Chen H, Zeng J, Wang B, Cheng Z, Xu J, et al. 2021. Structural characterization and antioxidant activities of bletilla striata polysaccharide extracted by different methods. *Carbohydrate Polymers* 266:118149
19. Ji X, Hou C, Yan Y, Shi M, Liu Y. 2020. Comparison of structural characterization and antioxidant activity of polysaccharides from jujube (*Ziziphus jujuba* Mill.) fruit. *International Journal of Biological Macromolecules* 149:1008–18
20. Li Z, An L, Zhang S, Shi Z, Bao J, et al. 2021. Structural elucidation and immunomodulatory evaluation of a polysaccharide from Stevia rebaudiana leaves. *Food Chemistry* 364:130310
21. Wang N, Jia G, Wang X, Liu Y, Li Z, et al. 2021. Fractionation, structural characteristics and immunomodulatory activity of polysaccharide fractions from asparagus (*Asparagus officinalis* L.) skin. *Carbohydrate Polymers* 256:117514
22. Lin X, Ji X, Wang M, Yin S, Peng Q. 2019. An alkali-extracted polysaccharide from *Zizyphus jujuba* cv. Muzao: structural characterizations and antioxidant activities. *International Journal of Biological Macromolecules* 136:607–15
23. Liu W, Xiao K, Ren L, Sui Y, Chen J, et al. 2020. Leukemia cells apoptosis by a newly discovered heterogeneous polysaccharide from *Angelica sinensis* (Oliv.) Diels. *Carbohydrate Polymers* 241:116279
24. Ayyash M, Abu-Jdayil B, Olaimat A, Esposito G, Itsaranuwat P, et al. 2020. Physicochemical, bioactive and rheological properties of an exopolysaccharide produced by a probiotic *Pediococcus pentosaceus* M41. *Carbohydrate Polymers* 229:115462
25. Huo J, Wu J, Zhao M, Sun W, Sun J, et al. 2020. Immunomodulatory activity of a novel polysaccharide extracted from *Huangshui* on THP-1 cells through NO production and increased IL-6 and TNF-α expression. *Food Chemistry* 330:127257
26. Shi Y, Ye YF, Zhang BW, Liu Y, Wang JH. 2021. Purification, structural characterization and immunostimulatory activity of polysaccharides from *Umbilicaria esculenta*. *International Journal of Biological Macromolecules* 181:743–751
27. Li F, Wei Y, Liang L, Huang L, Yu G, et al. 2021. A novel low-molecular-mass pumpkin polysaccharide: Structural characterization, antioxidant activity, and hypoglycemic potential. *Carbohydrate Polymers* 251:117090
28. Wang J, Hu S, Nie S, Yu Q, Xie M. 2016. Reviews on mechanisms of *in vitro* antioxidant activity of polysaccharides. *Oxidative Medicine and Cellular Longevity* 2016:5692852
29. Kawai T, Akira S. 2007. TLR signaling. *Seminars in Immunology* 19:24–32
30. Moresco EM, LaVine D, Beutler B. 2011. Toll-like receptors. *Current Biology* 21:R488–R493
31. Kawai T, Akira S. 2007. Signaling to NF-κB by Toll-like receptors. *Trends in Molecular Medicine* 13:460–469
32. Sun H, Zhang J, Chen F, Chen X, Zhou Z, et al. 2015. Activation of RAW264.7 macrophages by the polysaccharide from the roots of *Actinidia eriantha* and its molecular mechanisms. *Carbohydrate Polymers* 121:388–402
33. Sheng K, Wang C, Chen B, Kang M, Wang M, et al. 2021. Recent advances in polysaccharides from *Lentinus edodes* (Berk.): isolation, structures and bioactivities. *Food Chemistry* 358:129883
34. Wang M, Zhao S, Zhu P, Nie C, Ma S, et al. 2018. Purification, characterization and immunomodulatory activity of water extractable polysaccharides from the swollen culms of *Zizania latifolia*. *International Journal of Biological Macromolecules* 107:882–890